ARTICLE NO. 79-0044R

C80-051

20009
60006
80001

Effect of Intake Conditions on Supersonic Unstalled Flutter in Turbofan Engines

D. G. Halliwell*
Rolls-Royce Limited, Derby, U. K.

The nature of supersonic unstalled flutter, to which high tip speed, front stage fans of modern aircraft turbofan engines are susceptible, is introduced briefly. The effect of varying engine intake conditions of altitude, flight speed and ambient temperature are examined and test data is compared with theory. Some important flight conditions for minimum flutter margins in typical civil and military applications are outlined. The effect of engine intake type is then covered with respect to the degree of pressure distortion presented to the fan. A tentative relationship is derived between this distortion and flutter onset speed.

Nomenclature

A	= annulus area at fan face
D	= diametral node no.
D_A	= area distortion parameter
H	= fraction of blade height
K'	= 1000 ft altitude above SL
$KIAS$	= knots indicated airspeed
M	= flight Mach number
$m\sqrt{T}/P$	= intake massflow function
N_1	= fan rotational speed, rpm
n	= power or index of θ
P	= total pressure at fan face
$SL(S)$	= sea level (static)
T	= intake total temperature, K
TET	= turbine entry temperature
TO	= takeoff
δ	= damping logarithmic decrement
θ	= T relative to 288 K
ρ_s	= intake stagnation density, lb/ft^3

I. Introduction

THE basic characteristics of unstalled flutter have been examined previously in a number of papers on the subject.[1,2] Front stage fans of modern turbofan engines with part-span shrouds or clappers are particularly susceptible to this type of instability, because of their high tip speed, high aspect ratio, relatively lightweight blading, and the enhanced degree of coupling between blade flap and torsion modes provided by the shroud ring. The high-speed performance characteristics of such a fan stage are shown in Fig. 1. The supersonic flutter regime has a steep stress gradient, sensitive to speed and pressure ratio as illustrated. Its margin above the fan's design speed is of crucial importance, and both empirical correlations and unsteady work theoretical models are normally used to determine this margin.

The result of a typical theoretical analysis is shown in Fig. 2 for an unstalled high-speed condition on a shrouded fan assembly, using current unsteady aerodynamic theory.[3] The various nodal diameter vibration patterns of the assembly potentially can be excited in forward or backward rotating waves relative to the rotor. The aerodynamic damping logarithmic decrement of each mode is plotted against the vibration wave speed relative to the rotor. It is seen generally that the forward wave has the minimum damping and, therefore, is the least stable and that, in particular, flutter is most likely to occur in a 4-diameter mode rotating at about twice rotor speed. The backward wave, on the other hand, is stable and for the minimum mode is near-stationary relative to the casing.

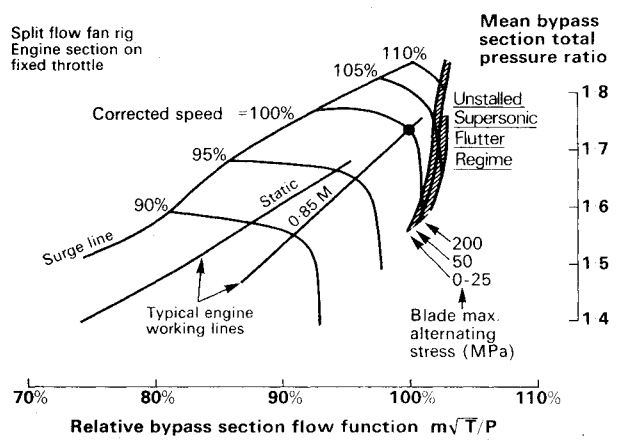

Fig. 1 Model fan characteristics showing stress boundaries of unstalled supersonic flutter.

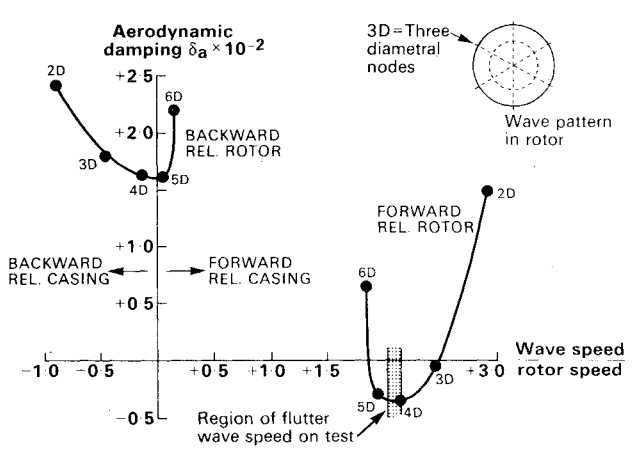

Fig. 2 Variation of aerodynamic damping and flutter wave speed with mode number (second family modes).

Presented as Paper 79-0044 at the AIAA 17th Aerospace Sciences Meeting, New Orleans, La., Jan. 15-17, 1979; submitted March 26, 1979; revision received Sept. 13, 1979.

Index categories: Nonsteady Aerodynamics; Aeroelasticity and Hydroelasticity; Engine Performance.

*Head of Aeroelastic Research, Aero Division.

Such a prediction as the above is governed by many input parameters. Some can be optimized, within other constraints, during the design of the fan itself. Others, such as the intake conditions, are determined by both the type of engine installation and the aircraft operating envelope. This paper examines some of the factors in this second category using, where possible, test data to illustrate the related flutter behavior.

Unless otherwise specified, the type of flutter referred to throughout is of the unstalled, supersonic variety.

II. Effect of Air Density

For a given fan rotor geometry, aerodynamic damping (log dec δ_a) is mainly dependent on interblade phase angle, blade relative Mach number, assembly mode frequency parameter (reduced frequency), and relative air density. The inter-blade phase angle is fixed for the mode in question. Mach number and frequency parameter are both functions of fan speed N_1 and to different degrees are dependent upon air temperature, giving a complex relationship between δ_a and corrected speed,[4] as referred to later.

On the other hand, δ_a is directly proportional to air density. Thus, for flutter onset, when δ_a is negative for a particular mode, we would expect the effect of reducing density to be favorable; i.e., at high altitude one would have to run the fan faster to reach flutter than on a sea level test bed (this will occur at a new combination of Mach number and frequency parameter). In addition, the gradient of stress-increase with speed when flutter has been reached will be more gradual at the lower density. These points should hold whether density is changed either by forward speed or by altitude, or by some combination of both.

On the face of it, this means that it is important to check out a demonstrator engine or development fan rig at the highest intake density condition likely to be encountered by the service derivative engine. In fact, this depends upon the particular aircraft operation to be fulfilled as Sec. IV will show.

A collection of test points is plotted in Fig. 3 in terms of fan corrected speed $N_1/\sqrt{\theta}$ at flutter onset against the intake stagnation air density ρ_s which is closely related to blade relative air density. Flutter has been defined at a low stress level, about 30 MPa, on or near the blade maximum stress position. More than one fan type is included in the correlation (each normalized to its design speed) which justifies the way in which it is used subsequently.

The expected effect of density is verified, but at the low density end the effect is more marked than at high density. This is partly due to the more favorable stress gradient referred to earlier. Density values for two different pairs of flight conditions are marked on Fig. 3, each pair having a different combination of altitude and flight Mach number for the same density. Points are included in the correlation for all these conditions showing that, within the data bandwidth, the density effect holds for both altitude and flight-speed variation.

Returning to the theoretical prediction of Fig. 2, the value of δ_a at flutter onset will be equal in magnitude to the logarithmic decrement of mechanical damping δ_m in the fan assembly. δ_m is a difficult quantity to determine, but its value will be reasonably independent of air density and also of fan speed within the restricted high-speed range we shall consider. δ_a, however, depends upon both these parameters. Thus, we have,

$$\delta_a = -\delta_m \text{ at flutter onset}$$

$$\propto \rho_s$$

$$= \text{function } N_1/\sqrt{\theta}$$

Knowing the theoretical relationship between δ_a and $N_1/\sqrt{\theta}$ at constant density, (e.g., Figs. 12 of Refs. 1 and 2,) we can construct curves of constant damping on the corrected speed/density diagram, to compare with the test data of Fig. 3. Note that, as stated earlier, we are dealing only with the case of negative aerodynamic damping, for which decreasing density is stabilizing.

This comparison is shown in Fig. 4, for a suitable range of δ_m. The shape of the constant damping curves is broadly similar to that of the test data with the slope increasing toward low density. A mechanical damping of about 0.008 gives general agreement with the test data over a reasonable density range, and is close to values which have been measured for the appropriate modes in laboratory and spinning pit testing.[5]

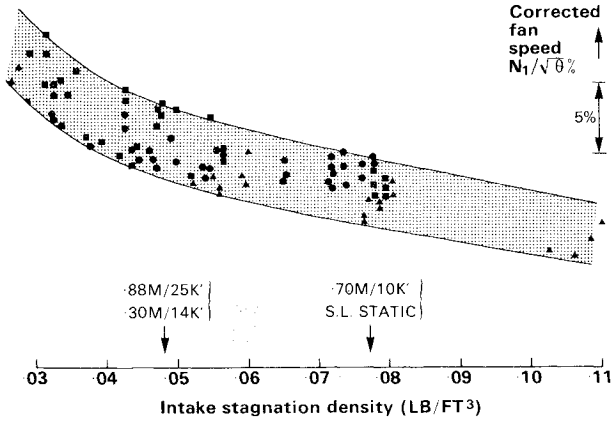

Fig. 3 Effect of intake air density on supersonic flutter onset—accumulated test data for ~ 30 MPa stress.

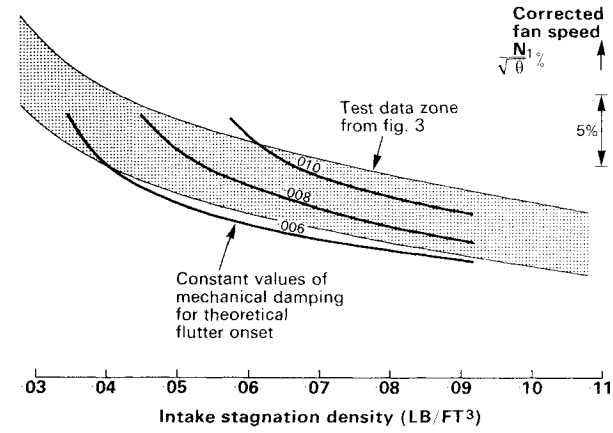

Fig. 4 Comparison of theoretical prediction of flutter onset with test data for varying air density.

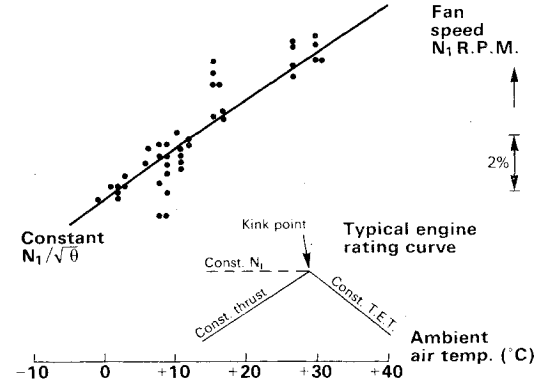

Fig. 5 Typical variation of flutter onset speed with ambient air temperature.

Extra confidence is thus lent to the theoretical prediction method.

Improvements in total damping measurement at varying air density and in the prediction accuracy of aerodynamic damping should permit a more thorough comparison to be made along the lines of Fig. 4 in the future.

III. Effect of Intake Air Temperature

The curve of corrected flutter onset speed with density established in Fig. 3 is not unique. It does not hold for large changes of air temperature at an otherwise constant operating condition. In fact, the spread of data in Fig. 3 is due partially to ambient air temperature variation.

Fig. 5 shows the variation of flutter speed with air temperature at sea level. The data obeys approximately a constant corrected speed law, i.e., $N_f/\theta^{0.5}$, which is typical for high-density operation. At low density, the temperature ratio index n can fall below 0.5, that is, flutter tends more toward a constant N_f relationship. The flutter boundary would then have a shallower slope than shown in Fig. 5. This is due to the complex interplay of two of the major parameters referred to earlier: Mach number relative to the blade (function of corrected speed) and frequency parameter (function of absolute speed).

The aforementioned intake temperature effect is seen to be very important when the engine thrust curve or rating curve is compared with the flutter boundary. Figure 5 shows a typical flat-rated engine thrust curve. Below the "kink-point" temperature the thrust is constant, which approximates to constant $N_f/\sqrt{\theta}$ for the fan. Above the kink-point, the turbine entry temperature (TET) is constant, causing a marked reduction of $N_f/\sqrt{\theta}$ as ambient temperature increases. Thus, for this type of engine rating curve, it is usually sufficient to examine the kink-point condition, to establish the minimum flutter margin at any particular altitude and flight speed. Clearly this will hold even more strongly when n falls below 0.5.

It should be noted that for an engine which does not have a "flat-rated" thrust curve, it may be necessary to introduce an N_f limiter or even an $N_f/\sqrt{\theta}$ limiter if there is a potential flutter problem on cold days.

IV. Operation of Aircraft

Having established the variation of the fan's flutter boundary with density and that (with certain provisos) the ambient temperature effect can be satisfied by taking the kink-point condition, we can examine the off-design operation of a derivative engine in a typical aircraft.

Taking first a civil transport aircraft, some important operating points are compared with the flutter boundary in Fig. 6. The highest fan corrected speed conditions to be considered are takeoff at high altitude and constant airspeed climb up to the aircraft's cruise altitude. In both cases it is seen that the slope of the flutter boundary with change of density lies in a favorable direction.

1) As takeoff altitude is increased, the air density reduces and the flutter speed recedes, although the margin between flutter and the engine rating does tend to reduce. Note that the points shown are alternative static takeoff conditions.

2) In the second case on Fig. 6 a continuous climb schedule is shown. As altitude is gained, the fan corrected speed increases until the stratosphere is reached. The slope of the flutter boundary also increases, such that there is a minimum flutter margin at or near to the top of climb just before a lower rating for cruise is selected.

It is part of the design process of a new engine to make sure that the margins just stated are adequate. Many factors are to be taken into account, such as thrust growth of the engine and deterioration of the fan in service, in determining what initial margins are acceptable. If the margins are unnecessarily large, a penalty may be incurred via excess fan weight.

Next we examine operation in a military aircraft. Here there are many more possibilities to consider than in the civil case, whether it be for a multi-role combat aircraft or for several aircraft designed for different specialized missions with a common engine. A selection of cases has been taken, as labeled in Fig. 7, plus normal takeoff, where each one is plotted on the corrected speed/density diagram. These are:

A) Subsonic climb at 0.75 M to 30,000 ft altitude.

B) Low level strike at 200 ft between 0.6 and 0.9 M.

C) Aerial combat in the range 0.9 M/15,000 ft to 1.4 M/25,000 ft.

D) Second segment climb with reheat for interception in the stratosphere at 1.6 M.

E) High-altitude reconnaissance at 50,000 ft.

The most obvious point from Fig. 7 is that high flight Mach number cases present the least problem from the flutter viewpoint, because the high ram intake temperature suppresses the fan corrected speed. The low level strike at high subsonic speeds (case B) might have been expected to be a problem because of the high intake stagnation density. However, the attendant high intake temperature ensures that here also the fan corrected speed is suppressed and the flutter margin is more favorable than, say, at the takeoff condition.

The highest fan corrected speeds occur at the top of the subsonic climb and in the slow-speed, high-altitude reconnaissance role. The latter is not a real problem because of the very low air density, but it might be preferable to impose an $N_f/\sqrt{\theta}$ limiter for performance reasons in this case and for flutter reasons in the subsonic climb case.

Therefore we see that the worst military flight conditions for supersonic flutter are not really different from the civil

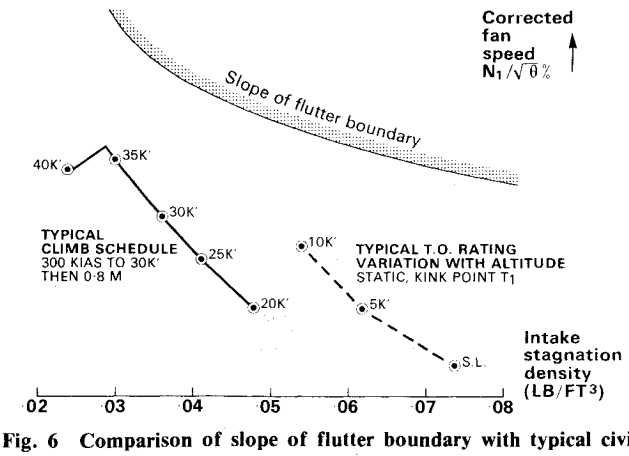

Fig. 6 Comparison of slope of flutter boundary with typical civil aircraft operation.

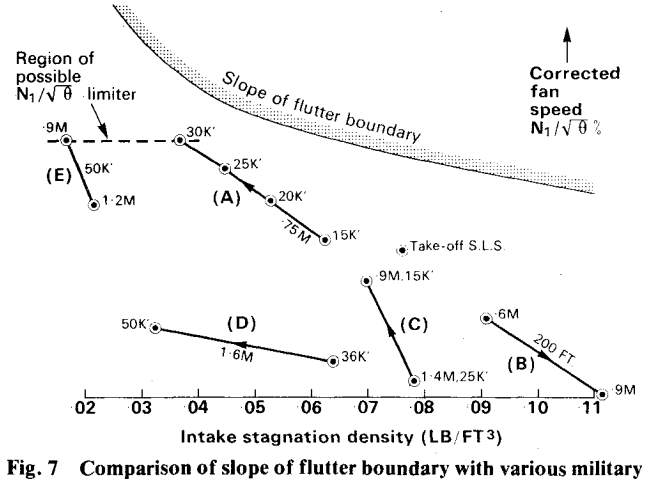

Fig. 7 Comparison of slope of flutter boundary with various military aircraft operations.

case. This is convenient from the point of view of developing a fan design which may be adopted in both fields.

V. Effect of Intake Distortion

So far we have considered operation with clean, uniform intake conditions, such as is provided by an airmeter in a test cell. However, we would expect the susceptibility of a fan to flutter to be influenced by the quality of the intake airflow as well as by its mean pressure and temperature.

It is fortunate that for once the laws of nature work in our favor. It is found that the most perfect case in terms of intake symmetry tends to give the lowest flutter onset speed. A measure of circumferential distortion, as found in real aircraft intakes, helps to suppress flutter. It is analogous to mechanical detuning, where physical asymmetry in the rotor can split the orthogonal components of the normal vibration mode and make their excitation at a common frequency more difficult than for the perfectly tuned rotor.[6] In the case of flutter, where the airflow provides the vibration energy input, asymmetry in the fan entry flow can provide detuning of an aerodynamic nature.

The effect is illustrated in Fig. 8, where averaged test data for a given fan behind different intake types is presented. The intake pressure recovery factor is used as a measure of the quality (in performance terms) of the intake. It is seen that the most efficient intakes are also the most flutter prone. The area of the "knee" of the curve is of special interest because this gives the biggest flutter improvement for the least intake loss.

As a further demonstration of this effect, the onset of flutter can be correlated in terms of a circumferential distortion parameter. At a given blade height H the circumferential total pressure factor presented to the fan face, $(P_{max.} - P_{min.})/P_{mean}$, has been calculated for various intake types, and plotted against H in Fig. 9. The maximum value of $P_{max.} - P_{min.}$ occurs typically near the fan tip for a pod intake, whereas for a buried installation it occurs much lower down the blade.

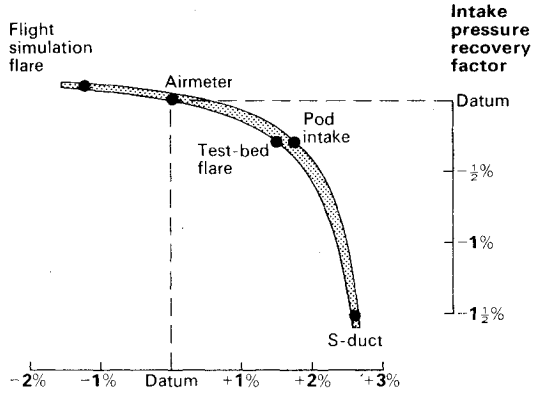

Fig. 8 Variation of average flutter onset speed with pressure recovery for different test bed intake types.

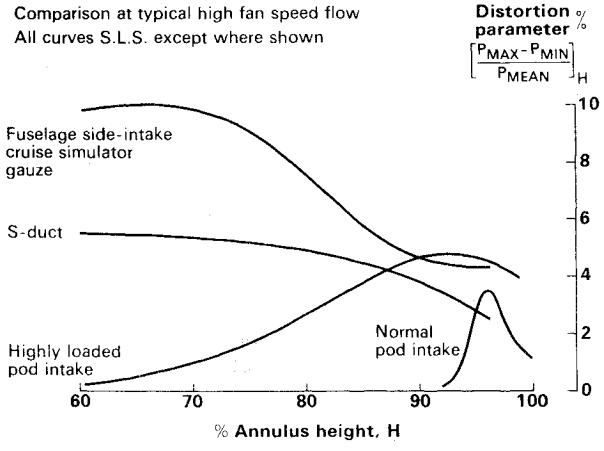

Fig. 9 Comparison of circumferential distortion parameter for different intake types.

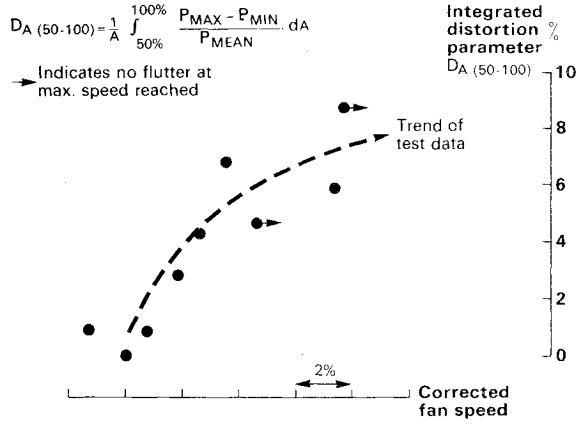

Fig. 10 Correlation of integrated distortion parameter with average flutter onset speed for different intake types.

It is necessary to integrate the aforementioned pressure factor over an appropriate part of the blade span. Because the maximum excitation forces and amplitudes occur near the blade tip, the outer part of the span is the most relevant; in fact the outer 50% of annulus area has been used here. Thus we have an area distortion parameter defined as

$$D_{A\,(50\text{-}100)} = \frac{2}{A}\int_{50\%}^{100\%}\left[\frac{P_{max.} - P_{min.}}{P_{mean}}\right]\cdot dA$$

where A is the fan inlet annulus area.

This parameter has been plotted in Fig. 10, for various intake test points, against the elevation of flutter onset speed above that measured with an airmeter. An arrow attached to certain points indicates that flutter was not present with that intake at the maximum speed reached.

The trend previously referred to is confirmed; that is, circumferential distortion can be beneficial to unstalled flutter. The implications of this are manifold. For example, it may be possible to design a variable geometry intake so as to improve flutter at certain conditions but not degrade engine performance at others. This would depend upon the proximity of stall and forced vibration criteria.

One positive outcome of this work is the general conclusion that customary rig and development engine testing with airmeters can be counted upon to give near to the lowest flutter speed. With aircraft-type intakes the flutter margins should certainly be no worse and could even be better. This is important as a lot of unnecessary test time and expenditure can be saved.

VI. Concluding Remarks

We have seen that supersonic flutter for different flight conditions can be correlated in terms of intake stagnation density, although the correlation is not unique with respect to ambient air temperature. Sea level testing will give close to the minimum corrected flutter speed with normal test cell intakes, whereas for real aircraft intakes the flutter speed will tend to be higher. It is shown that flutter onset speed can be correlated with either the intake efficiency or the circumferential distortion presented to the fan.

The minimum flutter margins in service will depend upon the engine's rating curves and the flight envelope of the aircraft. It is found that the worst cases tend to be at takeoff from high-altitude airfields and at maximum climb or con-

tinuous ratings near the top of the aircraft's lowest speed climb schedule. Normally it will be adequate to examine the kink-point temperature case. While these general observations can be used for project work, it is necessary to examine closely all the high corrected speed areas of any firm applications, in relation to the flutter boundary of the particular fan design adopted.

Acknowledgments

The author wishes to thank Rolls-Royce Limited, for permission to publish this paper. Views expressed therein are his own and not necessarily shared by the Company. This paper was originally presented to the AGARD Propulsion and Energetics Panel on October 26, 1978.

References

[1] Mikolajczak, Arnoldi, Snyder and Stargardter, "Advances in Fan and Compressor Blade Flutter Analysis and Predictions," *Journal of Aircraft*, Vol. 12, April 1975.

[2] Halliwell, D.G., "Fan Supersonic Flutter: Prediction and Test Analysis," Aeronautical Research Council R & M 3789, Nov. 1975.

[3] Nagashima, T. and Whitehead, D. S., "Aerodynamic Forces and Moments for Vibrating Supersonic Cascades of Blades," Cambridge University, CUED/A-Turbo/TR 59, 1974.

[4] Snyder, L.E., "Axial Fan/Compressor Flutter Design Principles," ASME 22nd International Gas Turbine Conference, March 1977.

[5] Hockley, B.S., Ford, R.A.J., and Foord, C.F., "Measurement of Fan Vibration using Double Pulse Holography," ASME 78-GT-111, April 1978.

[6] Ewins, D.J., "Vibration Characteristics of Bladed Disc Assemblies," *Journal of Mechanical Engineering Sciences*, Vol. 15, No. 3, June 1973, pp. 165-186.